The Astrophysical Journal Letters, 742:L34 (5pp), 2011 December 1 doi:10.1088/2041-8205/742/2/L34

DETECTION OF OUTFLOWING AND EXTRAPLANAR GAS IN DISKS IN AN ASSEMBLING GALAXY CLUSTER AT $z = 0.37$

Emily Freeland[1], Kim-Vy H. Tran[1,2], Trevor Irwin[1], Lea Giordano[2], Amélie Saintonge[3], Anthony H. Gonzalez[4], Dennis Zaritsky[5], and Dennis Just[5]
[1] George P. and Cynthia W. Mitchell Institute, Department of Physics and Astronomy, Texas A&M University, College Station, TX 77843, USA; freeland@physics.tamu.edu
[2] Institute for Theoretical Physics, University of Zürich, CH-8057 Zürich, Switzerland
[3] Max-Planck-Institut für Extraterrestrische Physik, Giessenbachstraße, D-85748 Garching, Germany
[4] Department of Astronomy, University of Florida, Gainesville, FL 32611, USA
[5] Steward Observatory, University of Arizona, Tucson, AZ 85721, USA
Received 2011 August 1; accepted 2011 October 26; published 2011 November 11

ABSTRACT

We detect ionized gas characteristics indicative of winds in three disk-dominated galaxies that are members of a super-group at $z = 0.37$ that will merge to form a Coma-mass cluster. All three galaxies are IR luminous ($L_{\rm IR} > 4 \times 10^{10}\ L_{\odot}$, SFR $> 8\ M_{\odot}\ {\rm yr}^{-1}$) and lie outside the X-ray cores of the galaxy groups. We find that the most IR-luminous galaxy has strong blueshifted and redshifted emission lines with velocities of $\sim \pm 200$ km s^{-1} and a third, blueshifted ($\sim$900 km s^{-1}) component. This galaxy's line widths (Hβ, [O III]λ5007, [N II], Hα) correspond to velocities of 100–1000 km s^{-1}. We detect extraplanar gas in two of the three galaxies with SFR $> 8\ M_{\odot}\ {\rm yr}^{-1}$ whose orientations are approximately edge-on and which have integral field unit (IFU) spaxels off the stellar disk. IFU maps reveal that the extraplanar gas extends to $r_h \sim 10$ kpc; [N II] and Hα line widths correspond to velocities of $\sim$200–400 km s^{-1} in the disk and decrease to $\sim$50–150 km s^{-1} above the disk. Multi-wavelength observations indicate that the emission is dominated by star formation. Including the most IR-luminous galaxy we find that 18% of supergroup members with SFR $> 8\ M_{\odot}\ {\rm yr}^{-1}$ show ionized gas characteristics indicative of outflows. This is a lower limit as showing that gas is outflowing in the remaining, moderately inclined, galaxies requires a non-trivial decoupling of contributions to the emission lines from rotational and turbulent motion. Ionized gas mass loss in these winds is $\sim 0.1\ M_{\odot}\ {\rm yr}^{-1}$ for each galaxy, although the winds are likely to entrain significantly larger amounts of mass in neutral and molecular gases.

Key words: galaxies: clusters: general – galaxies: evolution – galaxies: groups: general – galaxies: starburst

Online-only material: color figures

1. INTRODUCTION

Star formation can drive winds that transport gas to large distances from the parent galaxy. These outflows are nearly ubiquitous in infrared-luminous galaxies with star formation rates (SFRs) $> 10\ M_{\odot}\ {\rm yr}^{-1}$ (Rupke et al. 2005a). In the local universe, extraplanar emission line gas is observed in most galaxies with SFR $> 5\ M_{\odot}\ {\rm yr}^{-1}$ and in many cases there is evidence that this gas is outflowing (Veilleux et al. 2005). Simulations increasingly incorporate outflows in order to match a wide range of galaxy and intergalactic gas observables (Davé et al. 2011a, 2011b).

Starburst-driven outflows are composed of multi-phase gas. A tenuous, hot ($T \geqslant 10^6$ K) plasma created by stellar winds and supernovae ejecta is thought to carry most of the energy and metals in the outflow (Chevalier & Clegg 1985; Strickland & Heckman 2007) while neutral and molecular interstellar gas clouds entrained in the hot outflow contribute the majority of the mass (Sturm et al. 2011; Rupke et al. 2005b). Optical emission lines are thought to be produced by turbulent mixing layers on the surface of the cool entrained clouds as well as by diffuse ($T \sim 10^4$ K) ionized gas (Westmoquette et al. 2009).

The fate of the ejected multi-phase gas is likely to depend on the galaxy's mass as well as its environment. For example, massive, isolated galaxies are able to retain their hot, X-ray emitting gas reservoirs while low-mass galaxies are not (Mulchaey & Jeltema 2010). Hot gas winds from galaxies in groups and clusters may be confined by the dense intergalactic gas in these systems (Brown & Bregman 2000) or stripped away by it (Kawata & Mulchaey 2008; Hester 2006). Gas that is stripped will enrich the intergalactic medium with metals and entropy (Lloyd-Davies et al. 2000; Davis et al. 1999).

Most galaxies in the local universe are in groups (Geller & Huchra 1983; Eke et al. 2004) and groups are the building blocks of galaxy clusters (Boué et al. 2008; McGee et al. 2009). As outflows are common among star-forming galaxies, we expect to see many in group and field environments whose star-forming galaxy populations are comparable at $0.3 < z < 0.55$ (Tyler et al. 2011). We search for outflows from galaxies using integral field unit (IFU) spectroscopic observations of SG1120-1202 (hereafter SG1120), a system of four X-ray bright galaxy groups that will merge to form a cluster comparable in mass to Coma (Gonzalez et al. 2005).

We assume a flat cosmology with $H = 71$ km s^{-1} Mpc^{-1}, $\Omega_M = 0.27$, and $\Omega_{\rm vac} = 0.73$.

2. OBSERVATIONS

We used FLAMES/GIRAFFE (Pasquini et al. 2002) on the Very Large Telescope (PID: 082.B-0765) to take IFU spectroscopy of 60 SG1120 members in 2009 February. The instrument places 15 deployable IFUs across the 25′ field of view where each IFU is $3'' \times 2''$ and made of 20 spaxels ($0''.5$). Using the LR08 setup, the spectra cover a wavelength range of 822–940 nm with spectral resolution of 0.94 Å (31 km s^{-1} for Hα at $z = 0.37$). The FWHM of the point-spread function (PSF) ranged from $0''.66$ to $0''.97$.

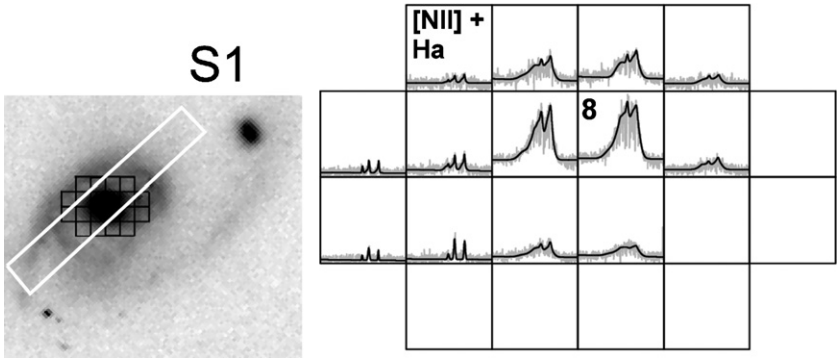

Figure 1. Left: *HST*/ACS F814W image with the FLAMES/GIRAFFE IFU ($3'' \times 2'' = 15$ kpc $\times$ 10 kpc) and single-slit ($1''$) footprints overlaid for source SG1120-S1. Right: the IFU data for S1 with spaxel 8 indicated.

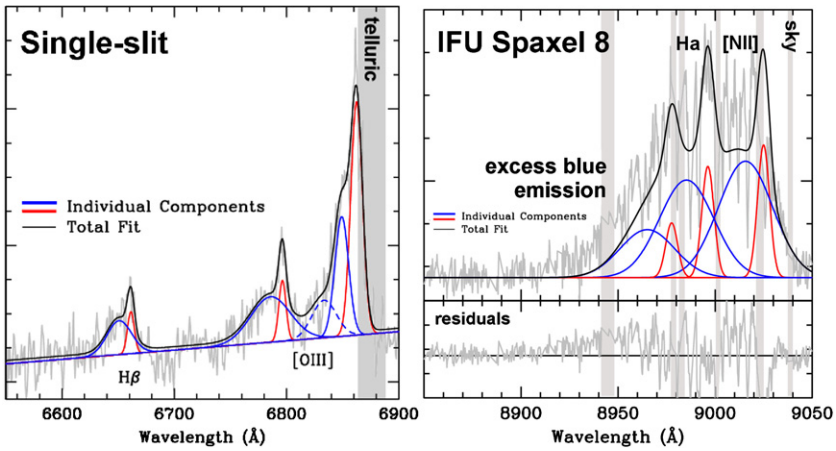

Figure 2. Left: single-slit spectrum centered on the nucleus of S1 ($z = 0.3692 \pm 0.0002$). The line-of-sight velocity offsets are $\sim \pm 200$ km s^{-1} and FWHM line widths are 200–1000 km s^{-1}. The red side of the [O III]λ5007 line is affected by telluric absorption. Forcing consistency between the profile shapes for the Hβ and [O III]4959 lines requires an additional broad component blueshifted by 900 km s^{-1} on the [O III]λ5007 line; this broad component is below our detection limit for Hβ and [O III]λ4959. The total fit is offset slightly high. Right: applying the two-component model to the blended spectrum in the brightest IFU spaxel indicates that the second blueshifted component (seen on the [O III]λ5007 line) is necessary to explain the excess blue emission.

(A color version of this figure is available in the online journal.)

We used the P3D software package (Sandin et al. 2010) to bias correct the CCD images, trace the spectra on the chip, flat field, correct for fiber-to-fiber transmission differences, and optimally extract the object spectra using multi-profile deconvolution. P3D also provides an error spectrum with each extracted object spectrum. We used IRAF to wavelength calibrate and produce spectra interpolated to a dispersion of 0.2 Å pixel^{-1}. The sky background was subtracted using spectra from 12 dedicated sky fibers on FLAMES. The IFU spectra are reassembled spatially and emission lines are fit with Gaussian components weighted by the associated error spectrum using custom IDL and Supermongo programs. The signal-to-noise ratio (S/N) is calculated for each line component in the fit and only components with S/N > 2 are included in our analysis. We fit the central blended IFU spaxels in SG1120-S1 by hand with IRAF/SPLOT using the three components in the [O III] lines from the multi-slit spectroscopy as a guide.

We have multi-slit spectroscopy with broader wavelength coverage of SG1120 (Tran et al. 2009). The multi-slits are all $1''$ wide and the two-dimensional spectra summed over the brightest $1''$ along the slit to generate the one-dimensional spectra. We measure systemic redshifts based on stellar absorption lines using the IRAF/RVSAO package and fit the Hβ and [O III] emission lines by hand with IRAF/SPLOT.

Key to our analysis is our extensive multi-wavelength data set of SG1120 that includes X-ray imaging from *Chandra*/ACIS (Gonzalez et al. 2005), total infrared luminosities from *Spitzer*/MIPS 24 μm imaging (Tran et al. 2009), *Hubble*/Advanced Camera for Surveys (ACS) F814W imaging, *Galaxy Evolution Explorer* (*GALEX*) UV imaging (Just et al. 2011), and a 1.4 GHz radio continuum map from the Very Large Array. The X-ray, UV, mid-infrared, and radio observations are critical for determining whether the velocity structure detected in the optical spectroscopy is driven by star formation or by active galactic nuclei (AGNs).

About a third of the SG1120 spectroscopically confirmed members (with $M_V < -20.5$) are detected in *Spitzer* 24 μm imaging with SFRs $\geqslant 3\ M_\odot$ yr^{-1} (Tran et al. 2009). Of these IR-detected galaxies 17 have SFR $> 8\ M_\odot$ yr^{-1} ($L_{8-1000\,\mu\mathrm{m}} > 4 \times 10^{10}\ L_\odot$, hereafter L_{IR}). We will discuss three of these galaxies, referred to arbitrarily as S1, S2, and S3 in this Letter.

3. EVIDENCE OF OUTFLOWING AND EXTRAPLANAR GAS IN GROUP GALAXIES

3.1. Luminous Infrared Galaxy: SG1120-S1

SG1120-S1 is a massive super-group galaxy with an infrared luminosity of $9 \times 10^{11}\ L_\odot$, i.e., nearly an ultraluminous infrared galaxy (ULIRG). Morphologically disturbed and connected to a nearby companion ($r_{\mathrm{proj}} \sim 25$ kpc) with a stellar tidal tail, SG1120-S1 is a poster child for merger-driven star formation (Figure 1). We find evidence of a strong gas outflow in

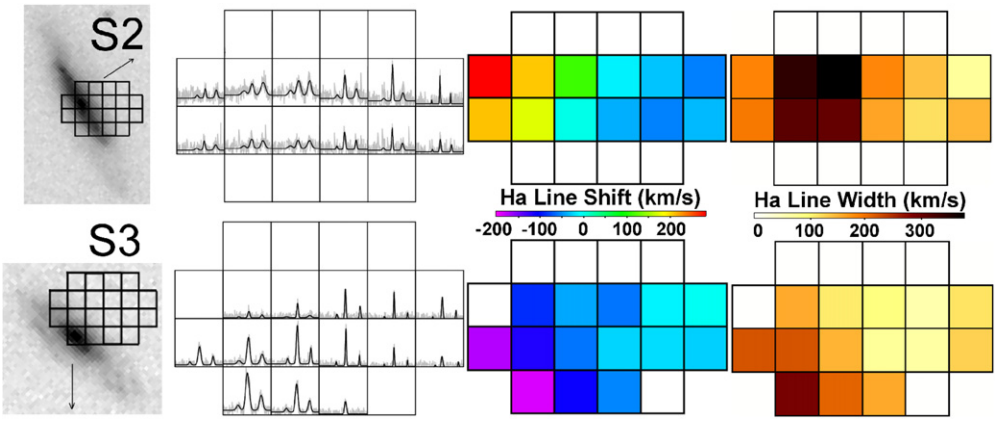

Figure 3. *HST*/ACS F814W image with the FLAMES/GIRAFFE IFU footprint ($3'' \times 2'' = 15$ kpc $\times$ 10 kpc) overlaid for sources SG1120-S2 and SG1120-S3. We center the IFU spaxel with the largest continuum value on the nucleus of the galaxy. The IFU footprint is populated with the spectra for each spaxel centered on the [N II] and Hα lines. The data are shown in light gray and our fit to the emission lines in black. Line shift and line width maps are shown. Errors on the line shifts (widths) are 68 km s^{-1} (5–15 km s^{-1}) and 73 km s^{-1} (5 km s^{-1}) for sources S2 and S3, respectively, following from the $\sim$100 km s^{-1} errors on the systemic velocity. Arrows indicate the direction toward the nearest group center, G4 for S2 and G2 for S3; group properties are detailed in Gonzalez et al. (2005) and Tran et al. (2009). Both S2 and S3 have extraplanar gas to at least $r_h \sim 10$ kpc above their disks.

(A color version of this figure is available in the online journal.)

Table 1
Galaxies

ID	α (J2000)	δ (J2000)	z	M_*[a] (10^{11} $M_\odot$)	$L_{1.4\ \mathrm{GHz}}$[b] (10^{22} W Hz^{-1})	$L_{8-1000\,\mu\mathrm{m}}$ (10^{11} $L_\odot$)	SFR$_{\mathrm{UV+IR}}$
S1	11 20 10.1	−12 10 12	0.3692	4.9	31 ± 0.2	8.8	150
S2	11 20 10.7	−12 11 04	0.3501	1.0	1.7 ± 0.2	0.54	9
S3	11 20 17.7	−11 57 57	0.3557	0.2	...	0.50	11

Notes.
[a] Details on the calculation of stellar masses, infrared luminosities, and star formation rates can be found in Tran et al. (2009).
[b] The 5σ point-source sensitivity is 1.1×10^{22} W Hz^{-1}.

SG1120-S1's nucleus in both our IFU and single-slit spectroscopy. The 1″ wide single-slit spectrum (Figure 2) samples the galaxy's inner 5 kpc and shows blueshifted and redshifted components in Hβ and [O III] that differ from the systemic velocity by $\sim \pm 200$ km s^{-1}. By forcing the profile shapes of the Hβ and [O III]4959 lines to be consistent, we find an additional broad component in the [O III]λ5007 line that is blueshifted by 900 km s^{-1}; note this broad component is much weaker than the other two components and thus below our detection threshold for both Hβ and [O III]λ4959. This second blueshifted component is also necessary when fitting the blended spaxels in the IFU data as the emission extends farther to the blue than would be expected for only the single blueshifted component. The line widths for Hβ, [O III]λ4959, and [O III]λ5007 are also broad and range from $\sim$1000 km s^{-1} for the blue component to $\sim$200 km s^{-1} for the red component. The combination of both blueshifted and redshifted components in the single-slit spectroscopic data indicates we may be viewing both sides of a bipolar outflow, an expanding bubble, or an outflow plus infalling tidal debris.

Our IFU spectroscopy maps the kinematics of the ionized gas as traced by [N II] and Hα, and reveals a complex of broad lines over multiple spaxels (Figure 2). There appears to be a single bright central spaxel that is broadened into neighboring spaxels by the telescope PSF as indicated by the unchanging red edge of the [N II]λ6583 line. We show the IFU data for illustration and use the single-slit data for all quantitative measurements of outflow dynamics. Beyond the galaxy's core ($r_{\mathrm{proj}} > 2.5$ kpc), the [N II]–Hα FWHM line widths decrease and the velocity offsets are consistent with rotation ($\pm$150 km s^{-1}). In spaxels with unblended lines we measure line ratios (log [N II]/Hα $\sim$ 0) that are best explained by shocked gas as is commonly seen in the extranuclear regions of ULIRGs (Monreal-Ibero et al. 2006). Note that the true gas velocities are likely to be higher because we are measuring only the motion along the line of sight.

Our multi-wavelength observations indicate that SG1120-S1 does not have a significant AGN component (Table 1): our 1.4 GHz and 24 μm measurements show that the galaxy falls on the infrared–radio relation for local star-forming galaxies (Yun et al. 2001). SG1120-S1 is X-ray detected but with an X-ray luminosity of $\sim 10^{42}$ erg s^{-1}, any embedded AGN must be Compton thick (Nardini & Risaliti 2011). For comparison, most U/LIRGs in this merger stage with similar L_{IR} are starburst or composite systems (Yuan et al. 2010). Star formation in U/LIRGs also tends to be concentrated in the central kiloparsec (Soifer et al. 2001, 2000) which corresponds to less than one spaxel in our IFU maps. The lines in the core spaxels are emitted primarily by gas that is participating in the outflow and their line ratios appear to be dominated by shock excitation as is commonly seen in starburst galaxies (Sharp & Bland-Hawthorn 2010). We conclude that SG1120-S1 is not AGN dominated, thus the strong gas outflows detected in both the IFU and single-slit spectroscopy are driven primarily by star formation.

3.2. Disk-dominated Members: SG1120-S2 and SG1120-S3

In the local universe extraplanar gas is detected in most highly inclined galaxies that have total infrared luminosities $>3 \times 10^{10}$ $L_{\odot}$ (SFR > 5 $M_{\odot}$ yr^{-1}; Veilleux et al. 2005). Our IFU observations include three such super-group galaxies and we discover that two have extraplanar emission with Hα and [N II] FWHM line widths of 50–150 km s^{-1} (Figure 3).

SG1120-S2 is a disk-dominated member viewed nearly edge-on that lies on the infrared–radio relation for local star-forming galaxies and is not detected with *Chandra* (Table 1). We detect [N II] and Hα emission in the disk and, surprisingly, also at projected heights of $r_h \sim 7.5$ kpc above the disk (Figure 3). In the spaxels sampling the galaxy disk, the log[N II]/Hα ratios of 0–0.2 are consistent with shocked gas and the measured line widths correspond to gas velocities of ∼300–400 km s^{-1}. In the extraplanar spaxels ($r_h > 5$ kpc), the log[N II]/Hα ratios of −0.2 to −0.4 are consistent with photoionization by starlight and the line widths correspond to gas velocities of ∼50–150 km s^{-1}. Our multi-wavelength observations indicate that as with SG1120-S1 the shocked gas in the central region of SG1120-S2 is due to star formation and not an AGN.

SG1120-S3 is also an inclined disk-dominated member (Figure 3) with comparable IR luminosity to SG1120-S2 (Table 1); it is detected neither in the radio nor in X-ray observations. The IFU maps show [N II] and Hα emission in both the disk and extraplanar spaxels ($r_h \sim 10$ kpc), and the line ratios are consistent with photoionization by starlight. The FWHM line widths correspond to velocities of ∼200–300 km s^{-1} in the disk spaxels and decrease to ∼50–150 km s^{-1} above the disk. With no signs of an AGN, the gas motion is most likely driven by the ongoing star formation.

In both group members where we detect extraplanar ionized gas, the emission lines vary in terms of relative velocity and width from spaxel to spaxel indicating that there is no PSF broadening in these sources. As with SG1120-S1, we measure only motion along the line of sight while the gas is likely to be primarily moving perpendicular to the disk, i.e., the true gas velocities are likely to be higher. We cannot determine a net flow direction for the extraplanar gas because the errors on the systemic velocity (∼100 km s^{-1}) for these two galaxies are large compared to the velocity shifts (∼10–65 km s^{-1}) in their extraplanar spaxels. However, we do confirm the existence of ionized gas at large scale heights above the disk of both members.

4. OUTFLOW GAS MASSES AND DISK GAS DEPLETION TIMESCALES

To determine what happens to the gas in these three members, we first estimate how much ionized gas is in the observed outflow. For SG1120-S1, using the Hβ lines from our single-slit data and the relation in Holt et al. (2006),[6] we assume case B recombination (Osterbrock 1989) and an electron density[7] of 100 cm^{-3} to estimate a total ionized gas mass of $M_{\rm H\,II} \sim 10^5$ $M_{\odot}$ in the two components of the Hβ line ($L_{\rm H\beta} = 2 \times 10^{39}$ erg s^{-1}). Next we estimate an outflow rate ($\dot{M}$) for the ionized gas by comparing the mass inferred from the Hβ emission to a dynamical timescale. Using the single-slit data we assume a radius of 1 kpc, consistent with the extent of the emission lines, and an outflow velocity of 900 km s^{-1} from the most blueshifted component on the [O III]λ5007 line, giving us $t_{\rm dyn} = R/V \sim 10^6$ yr. For SG1120-S1, $\dot{M} \sim M_{\rm H}/t_{\rm dyn} \approx 0.1$ $M_{\odot}$ yr^{-1} ; this is a lower limit because we cannot correct for extinction.

We stress that while the mass of ionized gas in the outflow is relatively modest, the outflow is likely to contain larger amounts of neutral and molecular gases. We cannot directly trace with our observations the multi-phase gas entrained in the outflow, but we note that SG1120-S1 has an intermediate $L_{\rm IR}$ between the LIRG and low-z ULIRG samples in Rupke et al. (2005b) for which typical outflows of neutral gas are, on average, ∼17–42 $M_{\odot}$ yr^{-1}. SG1120-S1 has a similar star formation rate and low AGN contribution to IRAS 13120-5453 for which *Herschel* observations reveal a molecular gas outflow rate of 130^{+390}_{-95} $M_{\odot}$ yr^{-1} (Sturm et al. 2011).

As SG1120-S1 loses gas through winds, it is also using up its reservoir of dense molecular gas through strong star formation. We can estimate the molecular gas content of these galaxies using the $L_{\rm FIR}$–$L_{\rm CO}$ relation (Sanders et al. 1991; Genzel et al. 2010). SG1120-S1 has a molecular gas reservoir of $\sim 9 \times 10^{10}$ $M_{\odot}$ (using the Galactic conversion factor). We calculate a star formation rate for this galaxy of 170 $M_{\odot}$ yr^{-1}, independent of its infrared emission, using its 1.4 GHz radio continuum luminosity (Bell 2003). Assuming it maintains this star formation rate and does not accrete new gas, SG1120-S1 will consume all of its molecular gas in ∼500 Myr. If, as indicated above, SG1120-S1 is expelling molecular gas at a rate comparable to its star formation rate then it will run out of the gas in half that time or 250 Myr.

For SG1120-S2 and SG1120-S3, we estimate the mass of ionized extraplanar gas using the Hα emission from our IFU observations (Nesvadba et al. 2006). Adopting the same electron density as for SG1120-S1 of 100 cm^{-3}, we estimate an ionized gas mass of 5×10^6 $M_{\odot}$ for SG1120-S2 and 1×10^7 $M_{\odot}$ for SG1120-S3. Assuming a moderate outflow velocity of ∼200 km s^{-1} consistent with winds from highly inclined galaxies in the local universe (Lehnert & Heckman 1996) the dynamical timescale for the outflow to reach 10 kpc is $t_{\rm dyn} \sim 5 \times 10^7$ yr, thus the mass-loss rate is $\dot{M} \sim 0.1$–0.2 $M_{\odot}$ yr^{-1}. Both galaxies are likely to have $\sim 8 \times 10^9$ $M_{\odot}$ of molecular gas and will consume all of this gas in the next ∼800 Myr if they maintain their current star formation rates and do not accrete new gas.

There are very few measurements of molecular outflow rates in galaxies which are not ULIRGs. In M82 ($M_{\rm tot} \sim 1 \times 10^{10}$ $M_{\odot}$; Sofue et al. 1992), whose $L_{\rm IR}$ is similar to SG1120-S2 and SG1120-S3, the molecular gas mass in the outflow is ∼30 $M_{\odot}$ yr^{-1} (Walter et al. 2002). It is $1.6^{+4.8}_{-1.2}$ $M_{\odot}$ yr^{-1} in NGC 253 ($L_{\rm IR} = 2 \times 10^{10}$ $L_{\odot}$, $M_* = 4 \times 10^{10}$ $M_{\odot}$; Bailin et al. 2011; Sturm et al. 2011). Thus, SG1120-S2 and SG1120-S3 may also be expelling significant quantities of molecular gas.

5. CONCLUSIONS

Using single-slit and IFU spectroscopy, we map the kinematics of ionized gas in galaxies that are part of an assembling galaxy cluster at $z = 0.37$. Here we present results on three IR-luminous, disk-dominated members that have ionized gas characteristics indicative of outflows.

SG1120-S1 is the most IR-luminous super-group member ($L_{\rm IR} = 9 \times 10^{10}$ $L_{\odot}$, SFR of 150 $M_{\odot}$ yr^{-1}). The Hβ and

[6] This estimate is subject to modulation by a filling factor due to the clumpiness of the gas and assumes a spherical outflow.

[7] Electron densities of 50–300 cm^{-3} are observed between 1 and 10 kpc for starburst superwinds (Heckman et al. 1990). We cannot measure the electron density directly because the [S II] lines are blended.

[O III]λ4959, 5007 emission lines in our single-slit data reveal gas that is blueshifted and redshifted from the systemic velocity by $\sim \pm 200\,\mathrm{km\,s^{-1}}$. We find a third, weaker component in the [O III]λ5007 emission that is blueshifted by $900\,\mathrm{km\,s^{-1}}$ but lies below the noise in the [O III]λ4959 and Hβ lines. The combination of both blueshifted and redshifted components in the single-slit spectroscopic data indicates that we are viewing both sides of a bipolar outflow or an expanding bubble, or an outflow plus infalling tidal debris.

In the local universe extraplanar gas is detected in most highly inclined galaxies that have SFRs $> 5\ M_\odot\ \mathrm{yr}^{-1}$ (Veilleux et al. 2005). Our IFU maps target four highly inclined super-group members with SFR $> 5\ M_\odot\ \mathrm{yr}^{-1}$ of which two show extraplanar gas. The IFU maps for SG1120-S2 and SG1120-S3 reveal extraplanar [N II] and Hα emission that is detected to at least ~7.5–10 kpc above the disk.

Our radio, IR, and X-ray observations indicate that all three galaxies are dominated by star formation. If they maintain their current star formation rates and do not accrete new fuel, they will run out of fuel in ~0.1–1 Gyr. We estimate that the wind in each of the three galaxies drives a relatively modest ionized gas mass flow of $\sim 0.1\ M_\odot\ \mathrm{yr}^{-1}$. As discussed in Section 4, these galaxies may be ejecting molecular gas at a rate comparable to their star formation rate.

It remains unclear how future star formation in these galaxies will be affected by these winds. In simulations, infalling galaxies continue to accrete gas for 0.5–1 Gyr after entering the larger halo (Simha et al. 2009) and a number of observed characteristics of satellite galaxies can be explained by a gradual reduction in star formation after infall (Weinmann et al. 2009). A recent *GALEX* study of the super-group S0 population finds no evidence for a recent strong star formation episode which stopped abruptly in these galaxies (Just et al. 2011). If SG1120-2 and SG1120-3 are S0 progenitors whose star formation will be quenched rapidly then they represent a new infalling population.

About a third (31 galaxies) of the SG1120 spectroscopically confirmed members (with $M_V < -20.5$) are detected in *Spitzer* 24 μm imaging with SFRs $\geqslant 3\ M_\odot\ \mathrm{yr}^{-1}$ ($L_{\mathrm{IR}} > 2 \times 10^{10}\ L_\odot$; Tran et al. 2009). Of these IR-detected galaxies 17 have SFR $> 8\ M_\odot\ \mathrm{yr}^{-1}$. Three are sources whose orientation is approximately edge-on and which have IFU spaxels off the stellar disk and we detect extraplanar gas in two of them, referred to here as S2 and S3. Including S1 we find that 18% of supergroup members with SFR $> 8\ M_\odot\ \mathrm{yr}^{-1}$ show ionized gas characteristics indicative of outflows. This is a lower limit as showing that gas is outflowing in the remaining moderately inclined galaxies requires a non-trivial decoupling of contributions to the emission lines from rotational and turbulent motion. Furthermore, 60% of the IR-detected members have an SFR $> 5\ M_\odot\ \mathrm{yr}^{-1}$ and, as a result, are likely to host a wind according to general estimates of the frequency of outflows (Veilleux et al. 2005).

Further identification and study of galactic winds in groups and clusters are needed to better understand their frequency and ability to transform galaxies and intergalactic gas as a function of environment.

K.T. acknowledges generous support from the Swiss National Science Foundation (grant PP002-110576).

REFERENCES

Bailin, J., Bell, E. F., Chappell, S. N., Radburn-Smith, D. J., & de Jong, R. S. 2011, ApJ, 736, 24
Bell, E. F. 2003, ApJ, 586, 794
Boué, G., Durret, F., Adami, C., et al. 2008, A&A, 489, 11
Brown, B. A., & Bregman, J. N. 2000, ApJ, 539, 592
Chevalier, R. A., & Clegg, A. W. 1985, Nature, 317, 44
Davé, R., Finlator, K., & Oppenheimer, B. D. 2011a, MNRAS, 416, 1354
Davé, R., Oppenheimer, B. D., & Finlator, K. 2011b, MNRAS, 415, 11
Davis, D. S., Mulchaey, J. S., & Mushotzky, R. F. 1999, ApJ, 511, 34
Eke, V. R., Baugh, C. M., Cole, S., et al. 2004, MNRAS, 348, 866
Geller, M. J., & Huchra, J. P. 1983, ApJS, 52, 61
Genzel, R., Tacconi, L. J., Gracia-Carpio, J., et al. 2010, MNRAS, 407, 2091
Gonzalez, A. H., Tran, K., Conbere, M. N., & Zaritsky, D. 2005, ApJ, 624, L73
Heckman, T. M., Armus, L., & Miley, G. K. 1990, ApJS, 74, 833
Hester, J. A. 2006, ApJ, 647, 910
Holt, J., Tadhunter, C., Morganti, R., et al. 2006, MNRAS, 370, 1633
Just, D. W., Zaritsky, D., Tran, K.-V. H., et al. 2011, ApJ, 740, 54
Kawata, D., & Mulchaey, J. S. 2008, ApJ, 672, L103
Lehnert, M. D., & Heckman, T. M. 1996, ApJ, 462, 651
Lloyd-Davies, E. J., Ponman, T. J., & Cannon, D. B. 2000, MNRAS, 315, 689
McGee, S. L., Balogh, M. L., Bower, R. G., Font, A. S., & McCarthy, I. G. 2009, MNRAS, 400, 937
Monreal-Ibero, A., Arribas, S., & Colina, L. 2006, ApJ, 637, 138
Mulchaey, J. S., & Jeltema, T. E. 2010, ApJ, 715, L1
Nardini, E., & Risaliti, G. 2011, MNRAS, 415, 619
Nesvadba, N. P. H., Lehnert, M. D., Eisenhauer, F., et al. 2006, ApJ, 650, 693
Osterbrock, D. E. (ed.) 1989, Astrophysics of Gaseous Nebulae and Active Galactic Nuclei (Mill Valley, CA: Univ. Science Books)
Pasquini, L., Avila, G., Blecha, A., et al. 2002, Messenger, 110, 1
Rupke, D. S., Veilleux, S., & Sanders, D. B. 2005a, ApJ, 632, 751
Rupke, D. S., Veilleux, S., & Sanders, D. B. 2005b, ApJS, 160, 115
Sanders, D. B., Scoville, N. Z., & Soifer, B. T. 1991, ApJ, 370, 158
Sandin, C., Becker, T., Roth, M. M., et al. 2010, A&A, 515, A35
Sharp, R. G., & Bland-Hawthorn, J. 2010, ApJ, 711, 818
Simha, V., Weinberg, D. H., Davé, R., et al. 2009, MNRAS, 399, 650
Sofue, Y., Reuter, H.-P., Krause, M., Wielebinski, R., & Nakai, N. 1992, ApJ, 395, 126
Soifer, B. T., Neugebauer, G., Matthews, K., et al. 2000, AJ, 119, 509
Soifer, B. T., Neugebauer, G., Matthews, K., et al. 2001, AJ, 122, 1213
Strickland, D. K., & Heckman, T. M. 2007, ApJ, 658, 258
Sturm, E., González-Alfonso, E., Veilleux, S., et al. 2011, ApJ, 733, L16
Tran, K., Saintonge, A., Moustakas, J., et al. 2009, ApJ, 705, 809
Tyler, K., Rieke, G. H., Wilman, D. J., et al. 2011, ApJ, 738, 56
Veilleux, S., Cecil, G., & Bland-Hawthorn, J. 2005, ARA&A, 43, 769
Walter, F., Weiss, A., & Scoville, N. 2002, ApJ, 580, L21
Weinmann, S. M., Kauffmann, G., van den Bosch, F. C., et al. 2009, MNRAS, 394, 1213
Westmoquette, M. S., Gallagher, J. S., Smith, L. J., et al. 2009, ApJ, 706, 1571
Yuan, T., Kewley, L. J., & Sanders, D. B. 2010, ApJ, 709, 884
Yun, M. S., Reddy, N. A., & Condon, J. J. 2001, ApJ, 554, 803